DESIGN AND PERFORMANCE OF AN AIRBORNE MULTIKILOHERTZ PHOTON-COUNTING, MICROLASER ALTIMETER

John Degnan, Jan McGarry, Thomas Zagwodzki, Phillip Dabney, Jennifer Geiger*
Code 920.3 (*Code 588)
NASA Goddard Space Flight Center
Greenbelt, MD 20771 USA
jjd@ltpmail.gsfc.nasa.gov, jan@ltpmail.gsfc.nasa.gov, tzagwodz@pop900.gsfc.nasa.gov, pdabney@ltpmail.gsfc.nasa.gov, jgeiger@pop700.gsfc.nasa.gov

Richard Chabot, Charles Steggerda
Honeywell TSI
7515 Missions Dr.
Lanham, MD 20706 USA
rchabot@pop900.gsfc.nasa.gov, Charles.Steggerda@Honeywell-TSI.com

Joseph Marzouk, Anderson Chu
Sigma Research and Engineering Corporation
9801 Greenbelt Rd., Suite 103
Lanham, MD 20706 USA
joe.marzouk@sigmaspace.com, andy.chu@sigmaspace.com

ABSTRACT

The present paper reports on the design and performance of a scanning, photon-counting laser altimeter, capable of daylight operations from aircraft cruise altitudes. In test flights, the system has successfully recorded high repetition rate, single photon returns from clouds, soils, man-made objects, vegetation, and water surfaces under full solar illumination. Following the flights, the signal was reliably extracted from the solar noise background using a Post-Detection Poisson Filtering technique. The passively Q-switched microchip Nd:YAG laser measures only 2.25 mm in length and is pumped by a single 1.2 Watt GaAs laser diode. The output is frequency-doubled to take advantage of higher detector counting efficiencies and narrower spectral filters available at 532 nm. The transmitter produces a few microjoules of green energy in a subnanosecond pulse at few kilohertz rates. The illuminated ground area is imaged by a 14 cm diameter, diffraction-limited, off-axis telescope onto a segmented anode photomultiplier. Each anode segment is input to one channel of "fine" range receiver (5 cm resolution), which records the times-of-flight of individual photons. A parallel "coarse" receiver provides a lower resolution (>75 cm) histogram of all scatterers between the aircraft and ground and centers the "fine" receiver gate on the last set of returns.

KEY WORDS: laser ranging**,** laser altimetry, photon-counting, microchip lasers, subnanosecond pulse, segmented anode photomultipliers, detector arrays, optical scanners

1. INTRODUCTION

Spaceborne laser altimeters typically use modest energy (50 to 100 mJ) solid state lasers, large telescopes (50 to 100 cm diameter), and high detection thresholds to achieve unambiguous surface returns with few or no “false alarms” resulting from solar background noise. Examples of such systems include the Mars Orbiter Laser Altimeter (Ramos-Izquierdo, L., et al, 1994), the Geoscience Laser Altimeter System (Abshire, J., 2000), and the Vegetation Canopy Lidar (Dubayah, R., et al, 1997). As a result of this conventional design philosophy, spacecraft prime power and weight constraints typically restrict spaceborne operations to low repetition rates on the order of a few tens of Hz which, at typical planetary orbital ground velocities of a few Km/sec, limits along-track spatial sampling to one sample every few hundred meters. There is great scientific interest in obtaining higher along-track resolution and/or better cross-track coverage, but achieving this capability through a simple scaling of the laser fire rate (power) is not practical.

It has been demonstrated theoretically (Degnan, 2000) that the conventional high Signal-to-Noise Ratio (SNR) approach to laser altimetry does not make efficient use of the available laser photons. The surface return rate of an orbiting altimeter can be increased by up to two orders of magnitude for a given laser output power by emitting the available photons in a high frequency (few KHz) train of low energy (< 1 mJ) pulses, as opposed to a low frequency train of high energy pulses, and by employing single photon detection (Degnan et al, 1998). Besides improving overall lidar efficiency, this mode of operation reduces the risk of internal optical damage to the laser, thereby improving long-term reliability, and makes the beam inherently more eyesafe to a ground-based observer. In addition, high return rates can be accomplished with much smaller telescope apertures on the order of 10 to 20 cm diameter. Indeed, the contrast of the terrain “signal” against the solar-induced noise background is actually enhanced through the use of small receive telescopes. Relatively simple onboard software algorithms, loosely based on post-detection Poisson filtering techniques previously used in lunar laser ranging (Abbott et al, 1973), can be employed to identify and extract the surface sampling data from solar background noise prior to onboard data storage or transmission of the data to a ground station.

The near order of magnitude reduction in telescope diameter greatly simplifies the mechanics of scanned systems and allows the use of relatively inexpensive, modest diameter

optical wedges or holographic optical elements to simultaneously scan both the transmit and receive beams for cross-track interrogation of the terrain while still maintaining a narrow receiver field of view for background noise suppression. In addition, since the volume and weight of a telescope and its support structure nominally varies as $D^{2.3}$, where D is the telescope diameter, a two order of magnitude reduction in weight and volume and a comparable reduction in fabrication cost can be realized.

Further unique performance enhancements are also possible when operating in a photon-counting mode. In conventional laser altimeters, multiple photons reflected from anywhere within the illuminated spot must be recorded by power-hungry waveform digitizers and deconvoluted using complex (and often fallible) algorithms in order to decipher the results and obtain a single range measurement. However, commercial and developmental photon-counting detectors now exist which are capable of providing centimeter level ranging resolution as well as angularly resolving the source of a single photon event within the receiver field-of-view. These devices can be realized either as segmented anode photomultipliers, available commercially from Hamamatsu with up to 10 x 10 pixels, or as Avalanche PhotoDiode (APD) arrays (Vasile, S., et al, 1997). With sufficiently high angular resolution of the single photon source, the measured range becomes nearly a point-to-point range measurement, i.e. from the internal altimeter reference point to a small area of uncertainty on the surface. The transverse spatial resolution is determined by the angular resolving power of the receiver/photodetector combination, which, for highly pixellated detectors, can be quite small compared to the total beam area on the ground. The vertical resolution is in turn limited by the laser pulsewidth, the timing capabilities of the range receiver, and the much-reduced residual spreading of the return waveform , or "Poisson generating function" in photon counting mode, caused by surface roughness and slope within this smaller zone of uncertainty. This ability to measure the near "point-to-point time-of-flight" of an individual photon removes much of the range ambiguity inherent in conventional altimeters and, as we shall demonstrate, produces high resolution 2D profiles and/or 3D topographic images.

We believe that a spaceborne microlaser altimeter, or "microaltimeter", can address many of the same Earth science issues as the aforementioned MOLA, GLAS, and VCL systems. Potential advantages of the microaltimeter approach include significantly greater spatial resolution in either the along-track or cross-track directions (or both) as well as greatly reduced demands on spacecraft resources such as prime power, volume and weight allocations, etc. Potential microaltimeter targets are the usual land, ice, and water surfaces as well as distributed or soft targets such as clouds, planetary boundary layers, tree canopies, and other vegetation (Ho, C., et al, 1995). The much-reduced signal levels of the microaltimeter relative to conventional altimeters are largely offset by a corresponding reduction in the detection threshold to about one photoelectron so that instrument sensitivity is largely maintained or even enhanced. As a result, geoscience applications include the development of a high resolution, high accuracy topographic database of land surfaces useful for studying hydrological runoff; the effects of clouds on radiation balance; changes in sea, lake, or reservoir levels; changes in ice sheet thickness; tree canopy heights and biomass assessment, etc. Applications to extraterrestrial science missions are both obvious and numerous and include the low power, high resolution topographic mapping of other planets, moons, asteroids, and comets within the Solar System. Commercial applications include aerial surveying of cities and towns and/or the generation of local topographic maps from aircraft cruise altitudes (6 to 12 km) using relatively small and inexpensive lasers. Even with their higher pulse energies, most conventional airborne laser altimeters must fly at altitudes below 1 km, which usually requires a special waiver from the FAA and makes the mapping of hilly or mountainous terrain both difficult and hazardous.

Under NASA's Instrument Incubator Program (IIP), the Goddard Space Flight Center has been developing an airborne multikilohertz microlaser altimeter ("microaltimeter") as a technology demonstration, which hopefully will lead to future space missions. Instrument development was initiated in December 1998. One engineering and two science flights were conducted in January, May, and August of 2001. The goals of the IIP program are to:

- Develop and demonstrate the necessary technologies and the operational and analytical software.
- Confirm the validity of the mathematical modeling and surface data extraction algorithms.
- Collect high spatial resolution topographic data over a variety of surfaces (land, ice, water, biomass, clouds) from a high altitude aircraft under both night and day conditions and evaluate its scientific usefulness relative to data from conventional laser altimeters.
- Demonstrate the technical and economic advantages of the microaltimeter concept for future Earth and planetary missions.

2. INSTRUMENT OVERVIEW

In order to improve the compatibility and portability of the instrument between different host aircraft, the microaltimeter has been designed to attach to a standard Lyca camera mount, commonly used in aerial surveying and photogrammetric missions and to operate at typical aircraft cruise altitudes between 6 and 12 km (20,000 to 40,000 ft).

The airborne microaltimeter is designed to operate at up to 10 kHz single photon sampling rates. Our choice of a 10 kHz fire rate was driven by several factors:

1. We wanted to match the return rates of the best conventional altimeters but with a lower power-aperture product instrument operating at higher altitudes in order to demonstrate the technical and economic advantages of the microaltimeter approach.
2. The 10 kHz rate allows system demonstrations to be carried out at aircraft cruise altitudes as high as 15 km (50,000 ft) without having to contend with multiple pulses in flight; this greatly simplifies the receiver design.
3. 10 kHz appeared to be a comfortable rate for modern data acquisition systems and would be compatible with the projected near term capabilities of space-qualified CPU's or Programmable Array Logic (PAL) processors.

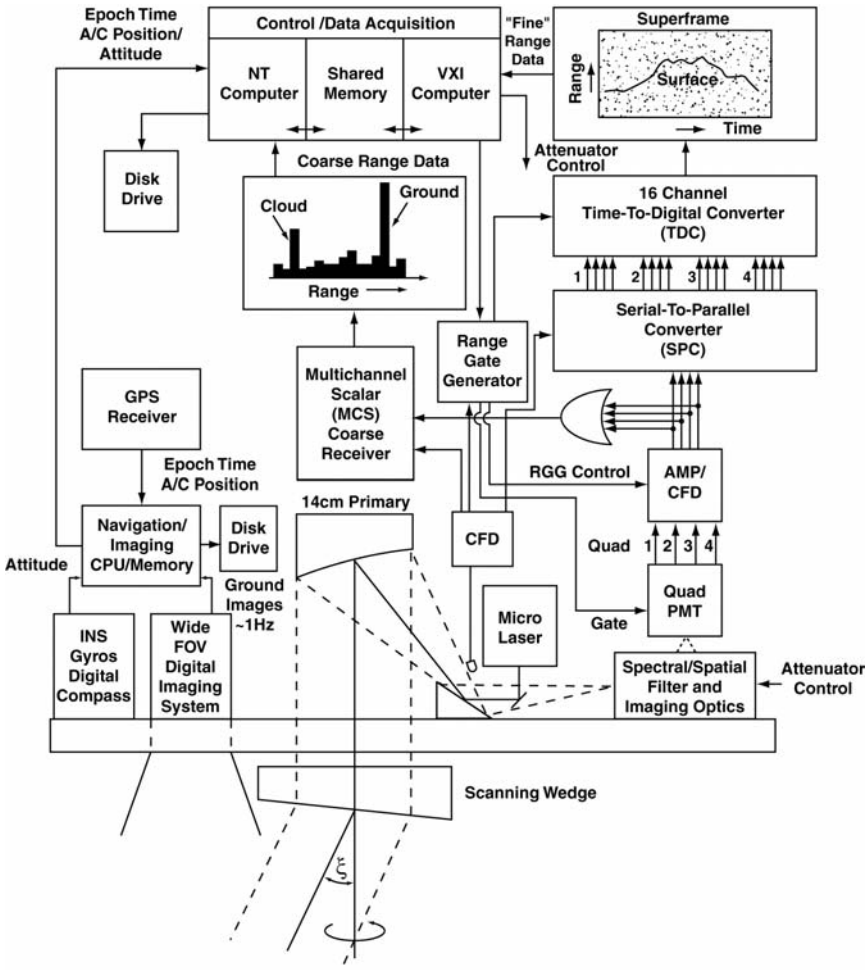

Figure 1: Block diagram of the IIP microlaser altimeter

A block diagram of the NASA IIP instrument is presented in Figure 1. In test flights carried out to date, a commercial microchip Nd:YAG laser, powered by a single 1.2 W CW laser diode and frequency doubled by a passive LBO nonlinear crystal, provides a low energy (few μJ), few kHz train of subnanosecond laser pulses at a visible green wavelength of 532 nm. The package, shown in Figure 2, contains a thermoelectric cooler, a 1.2 watt CW laser pump diode, the passively Q- switched Nd;YAG microchip laser, and an LBO nonlinear crystal for converting the infrared radiation to the visible.

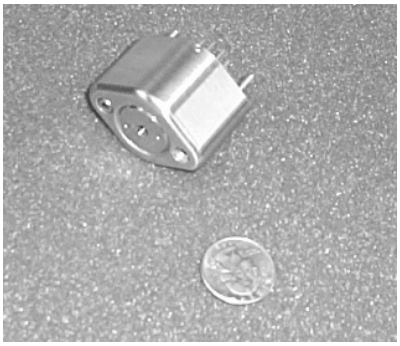

Figure 2: Commercial microlaser used in flight experiments compared to US quarter.

The microchip laser oscillator itself measures 2 mm x 2mm x 2.25 mm and consists of a Nd:YAG gain medium) segment diffusion-bonded to, or grown onto, a thin crystal of Cr^{4+}-doped YAG, which acts as a passive saturable absorber Q-switch and produces the sub-nanosecond pulses. The matching indices of refraction and diffused nature of the interface results in low internal optical loss. The monolithic laser resonator is formed by polishing opposite sides of the microchip optically flat and parallel and applying reflective coatings (Zayhowski, J., 1998). The resulting microlaser requires no active switching components and, because of the monolithic structure, can never go out of alignment. A small pick-off mirror injects the transmitter beam, following some initial divergence, into the central 5 cm of the common transmit/receive telescope, which uses a 20 cm off-axis parabola as the telescope primary mirror. Optical leakage from the outgoing laser pulse is sampled by a fast photodiode, which time-tags the start pulse with a Berkeley Nucleonics Corporation (BNC) Time-to-Digital Converter (TDC) and starts the range gate generator (BNC) Model B940). The TEM_{00} spatial mode quality (M^2 <1.3) of the end-pumped microlaser allows an extremely narrow transmit beam (< 20 arcsec) to be generated with a correspondingly small receiver FOV, which in turn reduces the solar noise

count rate. The laser spot diameter on the ground varies between 30 and 100 cm, depending linearly on aircraft altitude.

An internal computer-controlled aperture restricts the receiver to the central 14 cm of the primary or less. The receiver utilizes the remaining 87% of the available aperture that is not blocked by the injection mirror to gather photons reflected from the surface. Stray light rejection within the receive telescope and interface optics severely restricts the number of off-axis photons reaching the stop detector. The laser pickoff mirror effectively blocks the scattered return from within the aircraft and, combined with good spectral and spatial filtering, permits the detector to operate in an ungated mode, even in daylight.

The returning photons pass through spectral (0.4 nm) and spatial (~140 μrad) filters and are imaged onto a 2x2 element Hamamatsu Model R5900U metal channel dynode Photo-Multiplier Tube (PMT). Because the primary timing unit, the BNC Model B945 TDC, can accommodate up to 16 stop events (one in each of 16 channels), the receiver design permits 4 stop events to occur within the range gate for each of the 4 detector elements. Provisions have also been made in the design to incorporate either a single element Model R7400U (1 channel, 16 stops) or a 4x4 Model H6568 PMT (16 channels, 1 stop per pixel) as alternate detectors. Use of commercial segmented anode photomultipliers provides an inexpensive demonstration of the potential advantages of "quasi-imaging" or "point-to-point ranging". For example, at 12 km altitude where the ground beam diameter is about 120 cm, the 4x4 array allows the source of the received photon to be resolved within a roughly 30cm x 30 cm cell on the ground. In a 600 km Earth orbit, a roughly 20 m diameter beam would be dissected into 5 x 5 meter cells by a 4x4 array leading to a higher resolution ground "image". Of course, improved spatial resolution could be achieved through higher pixellation..

Each detector pixel output is input to a high speed amplifier/constant fraction discriminator (AMP/CFD) module (Phillips Scientific Model 6908). The CFD provides a fast timing pulse to both a "coarse" and a "fine" range receiver. The function of the coarse receiver is to simultaneously capture all of the "soft" scattering surface returns (e.g. clouds, boundary or fog layers) as well as the ground return and to provide an initial estimate of the range to the ground and near-ground scatterers (e.g. tree canopies and sub-canopies or man-made structures). The last "ground" return of the coarse receiver is used to center the range gate of the fine receiver in real time so that it can concentrate on resolving surface features with a minimum of noise background counts.

The "coarse" receiver is an EG&G Ortec Turbo- Multi-Channel Scalar (MCS) which bins all of the photons received over virtually the entire fire interval and creates a histogram of photon stop events. The best coarse range resolution of 75 cm is determined by the minimum MCS bin size of 5 nsec. Since this level of range accuracy is more than adequate for clouds or other meteorological layers and there is similarly no need for high spatial resolution in the transverse dimension, the "stop" outputs of all the pixels are ORed together at the input to the MCS.

The "fine" range receiver time-of-flight (TOF) measurement is determined by differencing the time tags of the laser fire ("start") event and the photon return ("stop") events in the TDC. Although the TDC has a timing resolution of 50 psec (7.5 mm), the range resolution of the fine receiver is limited by the detector impulse response to about 5 cm RMS. Furthermore, since the TDC is capable of measuring only one stop event per channel, the serial "stop" pulses (up to a maximum of four) from each of the four pixels must first be separated into parallel lines by a 4 channel Serial-to-Parallel Converter (SPC). The SPC output fans out to the 16 channels of the TDC, thereby preserving pixel identification.

In order of decreasing duration, individual gating pulses can be applied to the PMT, the MCS, and the TDC respectively by the multi-channel range gate generator as in Figure 1. In current flights of the prototype instrument, all photon “times-of-arrival” within the range gate, relative to the start pulse, are measured by the "fine" range receiver and recorded on the system hard disk for later analysis. However, our data extraction algorithms will be running in parallel to validate them in preparation for later operational flights, where software algorithms will identify the signal photons in flight and strip away most of the noise photons in near real-time.

There are three computers used in the flight system: the Ranging System Operator Interface (RGUI), the Ranging System Data Collector (RDATA), and the Navigational and Camera Control (NAV). A common timing reference is input to all three computers in the form of the current laser shot counter, which allows post-flight coordination of data recorded on separate computers.

The Ranging System Graphical User Interface (RGUI) is a 500 Mhz Pentium III processor running Windows NT 4.0. The system has 128 Mbytes of memory and two 13 Gbyte IDE Ultra ATA hard drives. One of the drives is used for system and program files; the other is mounted in a receiving frame for easy removal and will be used to record the flight data. The operator display is an LCD 20" rack mounted monitor with a pixel resolution of 1280 x 1024. The RGUI computer is responsible for operator interface, data logging, signal processing, and control of the EG&G Turbo-MCS Histogrammer. In addition this computer picks up a small data set from the NAV computer at 1 Hz using internet file sharing, and it reads 720 Kbytes of shared memory data from the RDATA computer at 1 Hz. Signal processing in RGUI provides visual feedback to the operator and can be used to provide control of the range window. All of the data is logged to the removable hard disk once per second. The amount of data recorded is approximately 3 Gigabytes per hour.

The basis of the RGUI software is NTGSE, which is a software package originally developed at GSFC for other missions. NTGSE has been modified for our application and has allowed a quicker software development cycle.

The Ranging System Data Collector (RDATA) is a 233 Mhz Pentium processor running DOS 6.22. The processor is an embedded module in a National Instruments VXI crate, which also contains a MXI interface to the RGUI computer (with 32Mbytes of shared memory), a digital I/O module (National Instruments DIO-128), and two Berkeley Nucleonics modules for ranging interface: the B940 digital delay generator (DDG) and the B945 16-channel time to digital converter (TDC). The embedded CPU contains 32 Mbytes of memory, a 4 Gbyte hard disk, as well as ethernet, SCSI, serial and parallel interfaces. RDATA uses an interrupt

from the TDC module at the end of each range gate to trigger the reading of the laser fire time, the 16 range returns, the scan angle, and the shot counter. Interrupts are generated at laser fire rates up to 10 Khz. Data is placed in a shared memory buffer for the RGUI computer to pick up when it can. The shared memory buffer is a circular buffer and currently holds 5 seconds worth of data. Commands from the RGUI to the RDATA computer are also sent across shared memory. These include the range delay, the size of the range window, and the scan commands and are picked up by RDATA at 2 Hz.

The instrument has been flown with and without the scanner operating in order to demonstrate both contiguous 2D linear profiling of the underlying terrain as well as the 3D mapping of larger swaths during a single pass of the aircraft. Because of the small size of the microaltimeter transmit/receive optics, an inexpensive optical wedge roughly 15 cm in diameter is rotated at rates up to 20 Hz to superimpose a circular scan (0.26 degree conical half angle) on the linear flight path motion. The rotating wedge simultaneously deflects both the transmitter beam and narrow receiver FOV Because of the small scan angle, the returning photons from the illuminated ground spot remain within the receiver FOV but, at higher aircraft altitudes, become increasingly displaced from the center due to the longer roundtrip transit time to the surface.

3. POST-FLIGHT DATA PROCESSING

In order to generate an accurate topographic map, it is essential for any laser altimeter that we know both the instantaneous position and attitude of the instrument on each laser fire in addition to the pulse time-of-flight and any fixed timing biases within the instrument. The latter bias can be determined by ranging to a target whose distance from the instrument reference point is well known. For the quasi-imaging and scanning microaltimeter, one must also make corrections based on the instantaneous off-nadir angle of the scanner and the X-Y coordinate (or pixel) which recorded the photon event.

Multiple GPS geodetic receivers are used (one in the aircraft and one or more on the ground) to provide post-flight dynamic differential positioning at the few decimeter level. The fixed offset vector between the GPS antenna phase center and the altimeter reference point in the aircraft reference frame is measured and corrected by three-axis attitude data to accurately locate the altimeter reference point in the Earth reference frame during flight. Instantaneous instrument attitude is provided by a three-axis fiber-optic gyro mounted directly on the altimeter optical bench and calibrated pre-flight. To counter or monitor gyro drift errors, independent updates of attitude are obtained in-flight by (1) a digital compass (for heading) supplemented by two collocated and orthogonal bench-mounted inclinometers and (2) repeatedly over-flying a set of four "ground stars", whose relative positions have been precisely located at the few mm level using geodetic GPS receivers. These "ground stars" are generally located near the center of the interrogated region to accommodate frequent overflights and arranged in a square or diamond pattern a couple of km on a side. Thus, when the aircraft is near the center of the pattern, they can all be viewed simultaneously by the wide FOV camera attached to the altimeter instrument, providing adequate angular resolution for updating the aircraft attitude at the few arcsecond level. The ground stars consist of small battery-powered Light Emitting Diode (LED) arrays, which are pulsed by the 1pps output of a GPS Timing Receiver. The onboard digital camera, boresighted with the range receiver and synchronized with the wide-angle ground star emission by the 1pps output of the onboard GPS receiver, then records the spectrally narrow images of the ground stars through a bandpass filter. The deviation of the ground stars from their predicted positions in the camera FOV, based on the few decimeter accuracy aircraft positioning, allows the instrument attitude to be updated post-flight with few arcsecond accuracy.

The instantaneous angular position of the scanning wedge is obtained by an encoder, time-tagged and recorded in the data file along with the ranging data. As mentioned previously, the detector pixel producing a given photon event is recorded by the "fine" range receiver and can be used to correct the measured elevation for the transverse location of the photon source within the ground spot.

To summarize, a "start" pulse and potentially one or more "stop" pulses (noise and/or signal counts) are recorded, for each laser fire, by the coarse and fine receivers, both of which can be viewed as correlation range receivers but with vastly different range gates and resolutions. A Post-Detection Poisson Filter (Degnan, J., 2000) identifies which cells in the coarse and fine receivers are most likely to contain signal counts. The photon times-of-flight for the echos selected as signal must then be subtracted from the aircraft altitude and corrected for pitch, roll, and yaw in order to determine the terrain heights. Additional corrections for the fixed offset of the GPS antenna from the instrument reference, the imposed off-nadir pointing due to the rotating scanner, attitude biases, and individual timing channel delays must also be made. Approximate X-Y locations, as determined by the pixellated or imaging detector, further allow more accurate placement of the measured terrain heights in the transverse dimension. The final analysis data product will be a three dimensional plot (and corresponding data files) of the terrain or sea heights for the scanned swaths obtained over multiple flight paths.

4. PRELIMINARY FLIGHT RESULTS

On January 4 and May 16 respectively of this year, the engineering and first science flight of the microaltimeter were respectively conducted on the NASA P3B aircraft housed at the Wallops Flight Facility (WFF). Both flights were conducted in full daylight under conditions of near maximum solar illumination. These flights have concentrated on target areas convenient to WFF which have already been accurately mapped by conventional altimeters, such as the area around Ocean City, Maryland, and Assateague Island, Virgina. The area offers a wide range of target types - tree canopies, water bodies, beach areas, and man-made structures. Barren terrain represents the simplest target for the microaltimeter and is useful in evaluating and optimizing the technique for future extraterrestrial planetary topographic mapping missions. Highly vegetated surfaces are much more complex and provide a test on whether or not the microaltimeter can successfully penetrate tree canopies to detect the ground and recover canopy and sub-canopy heights via statistical interpretation of the high repetition rate data. Towns and cities test the ability of the instrument and data processing algorithms to record and adapt to frequent and large elevation changes and assess its value as an aerial commercial surveying tool. Finally, overflights of beach

areas evaluate its capability for monitoring beach erosion and wave heights and for performing shallow water bathymetry at single photon levels. Ultimately, detailed comparisons between existing Digital Elevation Models, produced by repeated flights of the Wallops Airborne Topographic Mapper, and our own terrain measurements will be produced, giving point-to-point height differences and an overall measure of terrain difference.

Figure 3 provides a summary of the instrument parameters for the first engineering flight and some sample profiling data, taken between noon and 2 pm at three altitudes (3.3, 5.5, and 6.7 km). At the highest altitude of 6.7 km (22,000 ft), the mean signal strength per laser fire was computed to be less than 0.88 photoelectron (pe) per laser fire; at no altitude did the calculated mean signal exceed 3 pe per laser fire. Crosstalk between the receiver channels forced us to limit our observations to the first stop observed in any quadrant. Nevertheless, the system successfully generated high resolution profiles of buildings, tree canopies and underlying terrain, and even performed shallow water bathymetry over the Chesapeake Bay. Each of the figures shows approximately 2 seconds of altimetry data and is uncorrected for aircraft motion or attitude.

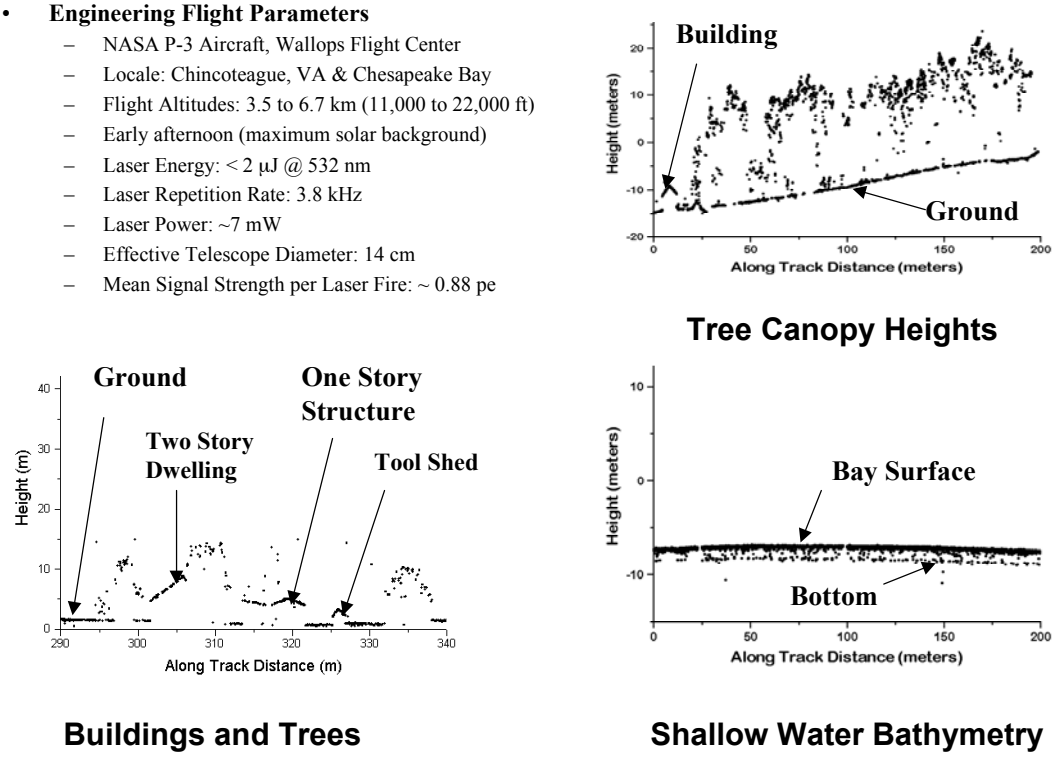

Figure 3: Engineering flight configuration plus sample profiling data from: small buildings and trees in the town of Chincoteague, VA, from 6.7 km altitude; tree lines and underlying terrain from 3.4 km altitude; and shallow water bathymetry over the Chesapeake Bay from 3.4 km altitude.

During the first science flight on the morning of May 16, both the scanner and the digital camera were available. Furthermore, the receiver crosstalk issues, which plagued the earlier engineering flight, were resolved. A single run over Assateague Island and Ocean City was made in both unscanned (2D profiling) and scanned (3D topographic) mode at a relatively low altitude of 1.6 km due to a failure in the laser's thermoelectric cooler which negatively impacted its performance. Figure 4 provides an example of the profiling data and corresponding digital images collected by the instrument. On the left hand side of the figure, we reproduce, from top to bottom: (1) a small segment of the aerial photograph taken by the onboard digital camera of a house in Ocean City, Maryland; (2) a ground photo of the house showing a tree in the rear yard (upper left of photo) , and a small shrub in the front of the house; and (3) approximately 0.3 seconds of altimeter data which clearly outlines the tree, rooftop, and shrub (plus some backyard shrubs not visible in the ground photo). Similarly, on the right hand side of the figure, we see two apartment houses (plus a portion of a third) outlined in the box in another aerial photo, followed by a ground image of the two buildings, and about one second of altimeter data. The ground photo shows a multi-tiered roof structure with single and dual chimney structures, which can also be clearly seen in the altimeter profiling data.

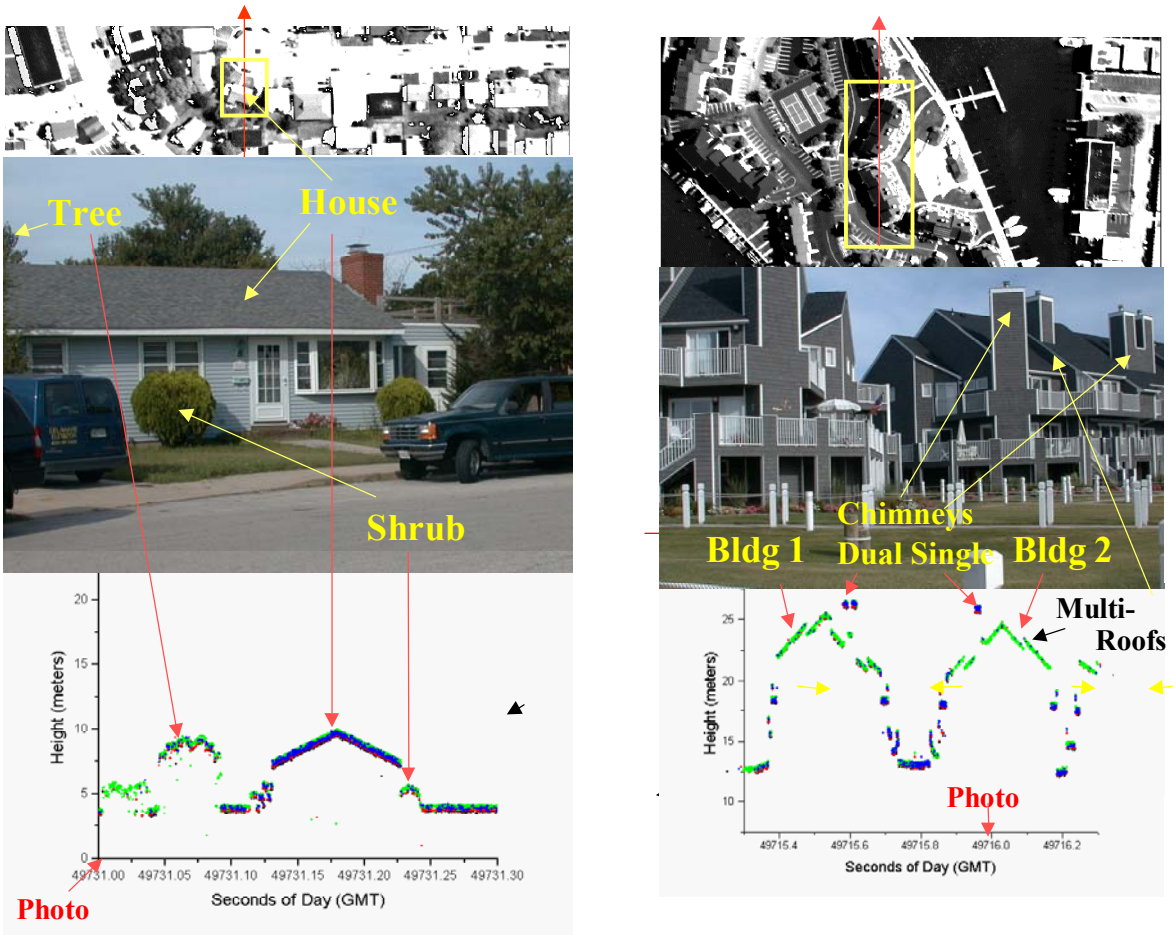

Figure 4: Profiling examples from the May 16 science flight showing (from top to bottom) an aerial photo taken by the onboard digital camera, a ground photo of the object, and the profile image as seen by the altimeter. The first example on the left is a single story home in a residential community while the second is a pair of apartment buildings with multi-tiered roofs and single and dual chimney stacks. The different color lidar points correspond to individual photons detected by different detector quadrants and have not been corrected for small differential channel delays to show the consistency between channels

5. CONCLUSIONS

Upcoming flights will make multiple passes over Ocean City and Assateague Island in order to build up a detailed topographic map which can then be compared to an existing Digital Elevation Model (DEM) of the region (Csatho, B., et al, 2001) to check the absolute accuracy of the instrument. The DEM was previously obtained by repeated flights of an existing, low altitude, laser altimeter - the Airborne Topographic Mapper- operated by Goddard's Wallops Flight Facility.

The productivity of the current instrument can be greatly improved through the use of somewhat higher power lasers and more efficient detectors. The average power of the commercial microchip lasers available for these experiments was quite low (7 to 20 mW). Passively Q-switched microchip Nd:YAG oscillators less than a cm in length and end-pumped via fiber bundles by a single linear diode array have produced output powers of greater than 1 W at 1064 nm (>600 mW at 532 nm) with repetition rates as high as 16 kHz and pulsewidths as short as 300 psec (Zayhowski, J., 1998). The commercial segmented-anode, metal dynode chain photomultiplier used in these experiments has a quantum efficiency of about 10% and an overall counting efficiency of 7% due to its internal geometry. Commercial tubes of this type with up to 100 (10x10) anodes are available from Hamamatsu. However, a segmented anode microchannel plate PMT with a GaAsP photocathode could potentially achieve a counting efficiency close to 40% at 532 nm without introducing the added complexity, expense, and long quenching times associated with avalanche photodiode (APD) arrays. By combining single photon ranging with efficient pixellated detectors and multistop, multichannel range receivers with low dead times (Degnan, J., 2000), the path to an efficient, few centimeter resolution, imaging 3D lidar seems clear. Unlike conventional laser altimeters, which rely on the deconvolution of complex multiphoton waveforms produced by a large laser ground spot, photon-counting lidars can provide efficient "point-to-point" ranging with excellent horizontal and vertical registration of multiple photon "events", even from vertically distributed or "soft" targets such as tree canopies.

REFERENCES

Abbott, R. et al, 1973. Laser observations of the Moon: Identification and construction of normal points for 1969-1971, The Astronomical Journal 78, pp. 784-793.

Abshire,J., et al, 2000. The Geoscience Laser Altimeter System (GLAS) for the ICEsat Mission , Proc. CLEO/QELS 2000, San Francisco, CA, May 7-12.

Csatho, B., et al, 2001. Creation of High Resolution, Precise Digital Elevation Models (DEM) of Ocean City and Assateague Island, these proceedings.

Dubayah, R. et al, 1997, The Vegetation Canopy Lidar Mission, Proceedings: Land Satellite Information in the Next Decade II: Sources and Applications, 1997, American Society for Photogrammetry and Remote Sensing, Bethesda, MD, December.

Degnan, J., 2000. Photon-counting multikilohertz microlaser altimeters for airborne and spaceborne topographic measurements, submitted to J. Geodynamics

Degnan, J. et al, 1998. Feasibility study of multikilohertz spaceborne microlaser altimeters, European Geophysical Society (EGS) Annual Symposium, Nice, France, April 20-24. (Abstract: Annales Geophysicae, Part I Society Symposia, Solid Earth Geophysics and Geodesy, Supplement 1 to Volume 16, p. C379)

Ho, C., et al, 1995. Volumetric measurement of plant canopies using laser ranging and mapping technique with a photon counting detector, Los Alamos National Laboratory, Internal Memorandum, NIS-2-95-206, Sept. 12.

Ramos-Izquierdo, L., et al, 1994. Optical system design and integration of the Mars Observer Laser Altimeter, Applied Optics, 33, pp. 307-322.

Vasile, S., et al, 1997. Photon detection with high gain avalanche photodiode arrays, IEEE Trans. Nuclear Science, 45, pp. 720-723.

Zayhowski, J., 1998. "Passively Q-switched microchip lasers and applications", Rev. Laser Eng., 26, pp. 841-846.